# Mitochondrial $Ca^{2+}$ removal amplifies TRAIL cytotoxicity toward apoptosis-resistant tumor cells via promotion of multiple cell death modalities

NATSUHIKO TAKATA[1], YOHEI OHSHIMA[1], MIKI SUZUKI-KARASAKI[1], YUKIHIRO YOSHIDA[1], YASUAKI TOKUHASHI[1] and YOSHIHIRO SUZUKI-KARASAKI[2,3]

[1]Department of Orthopedic Surgery, Nihon University School of Medicine, Tokyo 173-8610; [2]Plasma ChemiBio Laboratory, Nasushiobara, Tochigi 329-2813; [3]Division of Physiology, Department of Biomedical Sciences, Nihon University School of Medicine, Tokyo 173-8610, Japan

Received March 17, 2017; Accepted May 16, 2017

DOI: 10.3892/ijo.2017.4020

**Abstract.** $Ca^{2+}$ has emerged as a new target for cancer treatment since tumor-specific traits in $Ca^{2+}$ dynamics contributes to tumorigenesis, malignant phenotypes, drug resistance, and survival in different tumor types. However, $Ca^{2+}$ has a dual (pro-death and pro-survival) function in tumor cells depending on the experimental conditions. Therefore, it is necessary to minimize the onset of the pro-survival $Ca^{2+}$ signals caused by the therapy. For this purpose, a better understanding of pro-survival $Ca^{2+}$ pathways in cancer cells is critical. Here we report that $Ca^{2+}$ protects malignant melanoma (MM) and osteosarcoma (OS) cells from tumor necrosis factor (TNF)-related apoptosis-inducing ligand (TRAIL) cytotoxicity. Simultaneous measurements using the site-specific $Ca^{2+}$ probes showed that acute TRAIL treatment rapidly and dose-dependently increased the cytosolic $Ca^{2+}$ concentration ($[Ca^{2+}]_{cyt}$) and mitochondrial $Ca^{2+}$ concentration ($[Ca^{2+}]_{mit}$) Pharmacological analyses revealed that the $[Ca^{2+}]_{mit}$ remodeling was under control of mitochondrial $Ca^{2+}$ uniporter (MCU), mitochondrial permeability transition pore (MPTP), and a $Ca^{2+}$ transport pathway sensitive to capsazepine and AMG9810. $Ca^{2+}$ chelators and the MCU inhibitor ruthenium 360, an MPTP opener atractyloside, capsazepine, and AMG9810 all decreased $[Ca^{2+}]_{mit}$ and sensitized these tumor cells to TRAIL cytotoxicity. The $Ca^{2+}$ modulation enhanced both apoptotic and non-apoptotic cell death. Although the $[Ca^{2+}]_{mit}$ reduction potentiated TRAIL-induced caspase-3/7 activation and cell membrane damage within 24 h, this potentiation of cell death became pronounced at 72 h, and not blocked by caspase inhibition. Our findings suggest that in MM and OS cells mitochondrial $Ca^{2+}$ removal can promote apoptosis and non-apoptotic cell death induction by TRAIL. Therefore, mitochondrial $Ca^{2+}$ removal can be exploited to overcome the resistance of these cancers to TRAIL.

*Correspondence to:* Dr Yoshihiro Suzuki-Karasaki, Plasma ChemiBio Laboratory, 398 Takaatsu, Nasushiobara, Tochigi 329-2813, Japan
E-mail: suzuki-yoshihiro@opal.plala.or.jp
E-mail: suzuki.yoshihiro@nihon-u.ac.jp

*Key words:* TRAIL, $Ca^{2+}$ remodeling, mitochondrial $Ca^{2+}$, apoptosis, non-apoptotic cell death, malignant melanoma, osteosarcoma

## Introduction

Malignant melanoma (MM) and osteosarcoma (OS) are the representatives of aggressive tumors that are highly resistant to multidisciplinary treatment including chemo-, radio-, and immunotherapy (1,2). Apo2 ligand/tumor necrosis factor-related apoptosis-inducing ligand (Apo2L/TRAIL) is a member of the tumor necrosis factor superfamily. It has emerged as a promising cancer-selective anticancer drug since it exhibits potent cytotoxicity toward various cancer cell types with minimal cytotoxicity toward normal cells (3-5). Binding of TRAIL to two death receptors (DRs), TRAIL receptor (TRAIL-R)1/DR4 and TRAIL-R2/DR5 triggers the extrinsic and intrinsic apoptotic pathways (6,7). It also triggers pathways leading to other modes of cell death such as autophagy (8,9) and necroptosis (10,11). However, MM and OS are resistant to TRAIL-induced cytotoxicity, despite expressing DRs. In addition to their inherent resistance, the acquired resistance of MM and OS cells to the drug dampens TRAIL treatment (12). Consequently, the combined application of medicines that enable to reduce the TRAIL resistance is necessary for effective TRAIL therapy of these cancers.

$Ca^{2+}$ regulates many complicated cellular processes such as cell activation, proliferation, and death. Recently, $Ca^{2+}$ is emerging as a new target for cancer treatment. Various cancer cell types exhibit tumor-specific traits in $Ca^{2+}$ dynamics, which contribute to tumorigenesis, malignant phenotypes, drug resistance, increased proliferation, and survival (13-15). Growing body of evidence suggests that a variety of $Ca^{2+}$-permeable channels regulate $Ca^{2+}$ remodeling and survival in cancer cells (16). However, $Ca^{2+}$ promotes not only survival but also different modalities of cell death including apoptosis, necrosis, autophagy, and anoikis in cancer cells (17). Intracellular $Ca^{2+}$ overload was early thought to be a critical mediator of

necrotic cell death by leading to the increase in the permeability of the mitochondrial membrane (mitochondrial permeability transition) and the resulting dysfunction. $Ca^{2+}$/calpain, an intracellular $Ca^{2+}$-dependent cysteine protease, is activated by the rise in the cytosolic $Ca^{2+}$ concentration ($[Ca^{2+}]_{cyt}$) and critically involved in cancer cell apoptosis through the processing of the mitochondria-localized pro-apoptotic molecule, apoptosis-inducing factor (18,19). An excess, persistent rise in mitochondrial $Ca^{2+}$ concentration ($[Ca^{2+}]_{mit}$) increases the permeability of the inner membrane, thereby leading to release of pro-apoptotic proteins, the collapse of mitochondrial integrity, and activation of the intrinsic apoptotic pathway. Although the dual effect of $Ca^{2+}$ remodeling is thought to be due to the differences in the magnitude, timing, duration, and the space of the $Ca^{2+}$ surge generated (13), at present, no model can depict the dual role for $Ca^{2+}$ remodeling. Thus, drugs targeting overall $Ca^{2+}$ signals may modulate both pro-death and pro-survival pathways non-specifically, thereby compromising the antitumor effect. Therefore, it is necessary to characterize the cellular parameters and machinery that decide the two types of $Ca^{2+}$ signal and minimize the onset of the pro-survival $Ca^{2+}$ pathway by the therapy. To date, $Ca^{2+}$ remodeling in melanoma and osteosarcoma is poorly characterized, and the role for $Ca^{2+}$ in their malignant phenotypes and survival remains unclear.

In this study, we analyzed the impact of TRAIL on $Ca^{2+}$ remodeling in MM and OS cells and the possible role of $Ca^{2+}$ in their survival and TRAIL resistance. The results showed that acute TRAIL treatment modulates $Ca^{2+}$ dynamics and that $Ca^{2+}$ protects these tumor cells to TRAIL-induced apoptotic and non-apoptotic cell death. We also found that $Ca^{2+}$ remodeling in the mitochondria through mitochondrial uniporter (MCU), mitochondrial permeability transition pore (MPTP), and a $Ca^{2+}$ transport pathway sensitive to capsazepine and AMG9810 play a vital role in the protection. The findings suggest that mitochondrial $Ca^{2+}$ removal facilitates non-apoptotic cell death induction by TRAIL and may have therapeutic potential in the treatment of these TRAIL-resistant cancers.

## Materials and methods

*Materials*. Soluble recombinant human TRAIL was obtained from Enzo Life Sciences (San Diego, CA, USA). AMG9810, capsazepine, CGP-37157, atractyloside, thapsigargin (Tg), necrostatin-1, and the pan-caspase-inhibitor z-VAD-fluorometheylketone (z-VAD-FMK) were obtained from Sigma-Aldrich (St. Louis, MO, USA). All insoluble reagents were dissolved in dimethylsulfoxide and diluted with high glucose-containing Dulbecco's modified Eagle's medium (Sigma-Aldrich) supplemented with 10% fetal bovine serum (Sigma-Aldrich; FBS/DMEM) or Hank's balanced salt solution (HBSS) (pH 7.4) to a final concentration of <0.1% before use.

*Cell culture*. Human MM (A375, A2058) and OS (MG63, SAOS-2, HOS) cell lines were obtained from Health Science Research Resource Bank (Osaka, Japan) and cultured in FBS/DMEM in a 5% $CO_2$ incubator. Cells were harvested by incubating with 0.25% trypsin-EDTA (Thermo Fisher Scientific, Rochester, NY, USA) for 5 min at 37˚C.

*Cell growth and apoptosis measurements*. Cell growth was measured by WST-8 assay using the Cell Counting Kit-8 (Dojindo, Kumamoto, Japan), a colorimetric assay based on the formation of a water-soluble formazan product as previously described (20) with minor modifications. Briefly, cells ($8x10^3$/well) were seeded in 96-well plates and cultured with the agents to be tested for 72 h at 37˚C in a 5% $CO_2$ incubator. Then 1/10 volume of WST-8 reagent was added, incubated for 1 h at 37˚C and absorbance at 450 nm was measured using a microplate reader (ARVO MX, Perkin-Elmer Japan, Tokyo, Japan). Apoptotic cell death was quantitatively assessed by double-staining with fluorescein isothiocyanate (FITC)-conjugated Annexin V and propidium iodide (PI) as previously described (21). Briefly, cells ($2x10^5$/well) in 24-well plates were incubated with the agents to be tested for 24 h in 10% FBS-containing medium at 37˚C. The cells were then stained with FITC-conjugated Annexin V and PI using a commercially available kit (Annexin V FITC Apoptosis Detection kit I; BD Biosciences, Tokyo, Japan). The stained cells were evaluated in the FACSCalibur and analyzed using CellQuest software (BD Biosciences). Four cellular subpopulations were assessed: viable cells (Annexin $V^-/PI^-$); early apoptotic cells (Annexin V+/PI-); late apoptotic cells (Annexin $V^+/PI^+$); and necrotic/damaged cells (Annexin $V^-/PI^+$). Annexin $V^+$ cells were considered to be apoptotic cells.

*$Ca^{2+}$ measurements*. Changes in $[Ca^{2+}]_{cyt}$ and $[Ca^{2+}]_{mit}$ were measured using the cytosol $Ca^{2+}$-reactive fluorescence probe Fluo 4-AM and mitochondrial $Ca^{2+}$-reactive fluorescence probe rhod 2-AM (both were obtained from Dojindo), respectively as previously described (22). To improve its mitochondrial localization, rhod 2-AM was reduced to the colorless, nonfluorescent dihydrorhod 2-AM by sodium borohydride, according to the manufacturer's protocol. Cells were loaded with 4 $\mu$M each of Fluo 4-AM or dihydrorhod 2-AM for 40 min at 37˚C and washed with HBSS. Then, the cells ($1x10^6$/ml) were resuspended in HBSS in 96-well plates. The cells were manually added with the agents to be tested. Then, the cells were measured for fluorescence at 5 sec intervals up to 3 min in a microplate reader (Fluoroskan Ascent, Thermo Fisher Scientific) with excitation and emission at 485 and 538 nm (for Fluo 4-AM), respectively and 542 and 592 nm (for rhod 2-AM), respectively. For $Ca^{2+}$-independent experiments, cells were suspended in HBSS supplemented with 1 mM EGTA in place of 1 mM $CaCl_2$.

*Caspase-3/7 activation, membrane integrity, and cell death assay*. Caspase-3/7 activation, membrane integrity, and cell death were simultaneously measured by Muse™ Cell Analyzer (Merck Millipore, Darmstadt, Germany) using Muse Caspase-3/7 kit. Briefly, cells ($1x10^5$/ml) in 24-well plates were treated with the agents to be tested for 24 h in 10% FBS/DMEM at 37˚C and then stained with a novel Caspase-3/7 reagent NucView™ and 7-amino-actinomycin D (7-AAD), a dead cell marker in the kit. 7-AAD is excluded from healthy and early apoptotic cells, while permeates late apoptotic and dead cells. Consequently, four populations of cells can be distinguished by the kit; Live cells: $Caspase^-/7\text{-}AAD^-$; early apoptotic cells: $Caspase^+/7\text{-}AAD$-; late apoptotic/dead cells: $Caspase^+/7\text{-}AAD^+$; necrotic cells: $Caspase^-/7\text{-}AAD^+$.

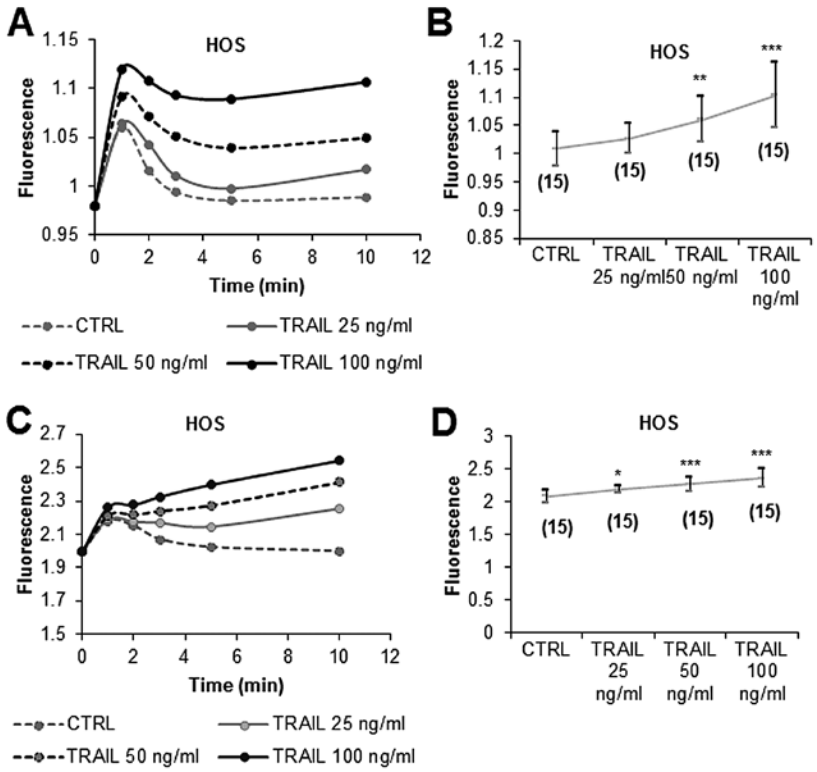


Figure 1. TRAIL modulates $Ca^{2+}$ dynamics in malignant cells. HOS cells were loaded with 4 $\mu$M Fluo 4-AM (A and B) and dihydrorhod 2-AM (C and D), respectively, for 40 min at 37˚C, washed with HBSS. The dye-loaded cells ($1x10^6$/ml) were resuspended in the $Ca^{2+}$-containing medium in 96-well plates. After addition of 25, 50, or 100 ng/ml TRAIL to the cells, fluorescence was immediately measured in triplicate in a microplate reader at 0, 1,2,3,5,10 min with excitation and emission at 485 and 538 nm (for Fluo 4-AM), respectively and 542 and 592 nm (for dihydrorhod 2-AM), respectively. The data show means ± SD in a representative experiment (N=3). (B and D) Data were analyzed by ANOVA followed by the Tukey's post-hoc test. $^{*}$P<0.05; $^{**}$P<0.01; $^{***}$P<0.001 vs. control (CTRL). The number of parentheses represents the data analyzed.

*Statistical analysis*. Data were analyzed by one-way analysis of variance (ANOVA) followed by the Tukey's post-hoc test using an add-in software for Excel 2016 for Windows (SSRI, Tokyo, Japan). All values are expressed as means ± SD, and P<0.05 was considered to be significant.

## Results

*Analyses of $Ca^{2+}$ dynamics in MM and OS cells stimulated with TRAIL*. To determine the impact of TRAIL on $Ca^{2+}$ dynamics in tumor cells, we measured the effect of TRAIL on $[Ca^{2+}]_{cyt}$ and $[Ca^{2+}]_{mit}$ in osteosarcoma cells in parallel. Treatment with soluble recombinant human TRAIL resulted in a robust increase in $[Ca^{2+}]_{cyt}$ in HOS cells in a dose-dependent manner (Fig. 1A and B). The increase occurred rapidly (within minutes) and persistently (lasted at least for 10 min). TRAIL at concentrations of ≥50 ng/ml had a significant effect in parallel with the cytotoxic effect. In parallel, $[Ca^{2+}]_{mit}$ was increased in a dose-dependent manner (Fig. 1C and D). Depending on the cellular conditions, $[Ca^{2+}]_{mit}$ was elevated maximally at 50 ng/ml, and higher concentrations of TRAIL had a smaller effect. We observed similar results in an array of MM and OS cells including SAOS-2, MG63, A375 and A2058 cells (not shown).

*The MCU inhibitor Ruthenium 360 (Ru360) suppresses mitochondrial $Ca^{2+}$ load in MM and OS cells*. MCU is a major molecular machinery responsible for the physiological $Ca^{2+}$ load into the mitochondrial matrix (23). The role of MCU in mitochondrial $Ca^{2+}$ remodeling has been studied in few tumor cells including breast cancer cells (24) and neuroblastoma cells (25). Since the role of MCU in mitochondrial $Ca^{2+}$ remodeling in MM and OS cells is unknown, we examined the impact of MCU-specific agents on their mitochondrial $Ca^{2+}$ dynamics. The MCU inhibitor Ru360 caused a significant decrease in $[Ca^{2+}]_{mit}$, while the mitochondrial $Na^{+}$-$Ca^{2+}$ exchanger (NCLX) inhibitor CGP-37157 increased $[Ca^{2+}]_{mit}$ in HOS and SAOS-2 cells (Fig. 2A and B). EGTA and the mitochondrial permeability transition pore (MPTP) inhibitor cyclosporine A (CysA) significantly decreased $[Ca^{2+}]_{mit}$ in HOS cells, but not in SAOS-2 cells (Fig. 2A and B). On the other hand, atractyloside, an MPTP opener, significantly reduced $[Ca^{2+}]_{mit}$ in both MM and OS cells (Fig. 2C and D), indicating that $Ca^{2+}$ extrusion through the MPTP participates in regulating $[Ca^{2+}]_{mit}$.

*Capsazepine and AMG9810 reduce $[Ca^{2+}]_{mit}$ cooperatively with TRAIL in MM and OS cells*. We found that capsazepine and AMG9810 modulated mitochondrial $Ca^{2+}$ dynamics in MM and OS cells. AMG9810 alone at concentrations ranging from 1 to 10 $\mu$M decreased $[Ca^{2+}]_{mit}$ in A2058 cells in a dose-dependent manner (Fig. 3A). Capsazepine alone reduced $[Ca^{2+}]_{mit}$ maximally at 1-3 $\mu$M (Fig. 3B). When used with TRAIL and AMG9810 together, $[Ca^{2+}]_{mit}$ was dropped to the level lower than that observed with each agent alone (Fig. 3A). Meanwhile, capsazepine enhanced the effects of TRAIL on $[Ca^{2+}]_{mit}$ with

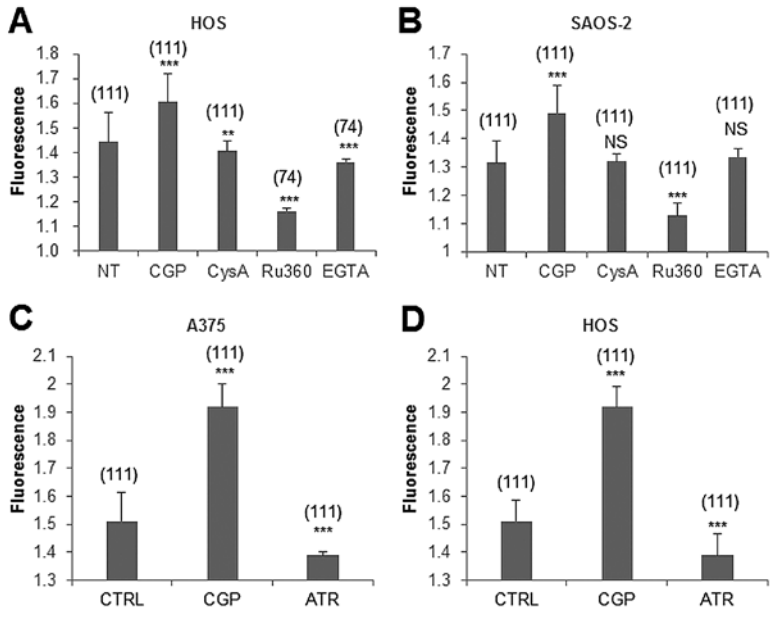


Figure 2. The mitochondrial $Ca^{2+}$ dynamics is regulated by MCU and MPTP. Dihydrorhod 2-AM-loaded HOS (A and D), SAOS-2 (B), and A375 cells (C) were resuspended in the $Ca^{2+}$-containing medium in 96-well plates. The cells were added with 10 $\mu$M CGP-37157 (CGP), 1 $\mu$M cyclosporine A (CysA), 1 $\mu$M Ruthenium 360 (Ru360), or 0.5 mM EGTA (A and B) or 10 $\mu$M CGP or 5 $\mu$M atractyloside (ATR) (C and D). Then, fluorescence was immediately monitored in triplicate at 5 sec intervals up to 3 min. The data show means ± SD in a representative experiment (N=3). Data were analyzed by ANOVA followed by the Tukey's post-hoc test. $^{**}$P<0.01; $^{***}$P<0.001; NS, not significant vs. non-treated control (NT). The number of parentheses represents the data analyzed.

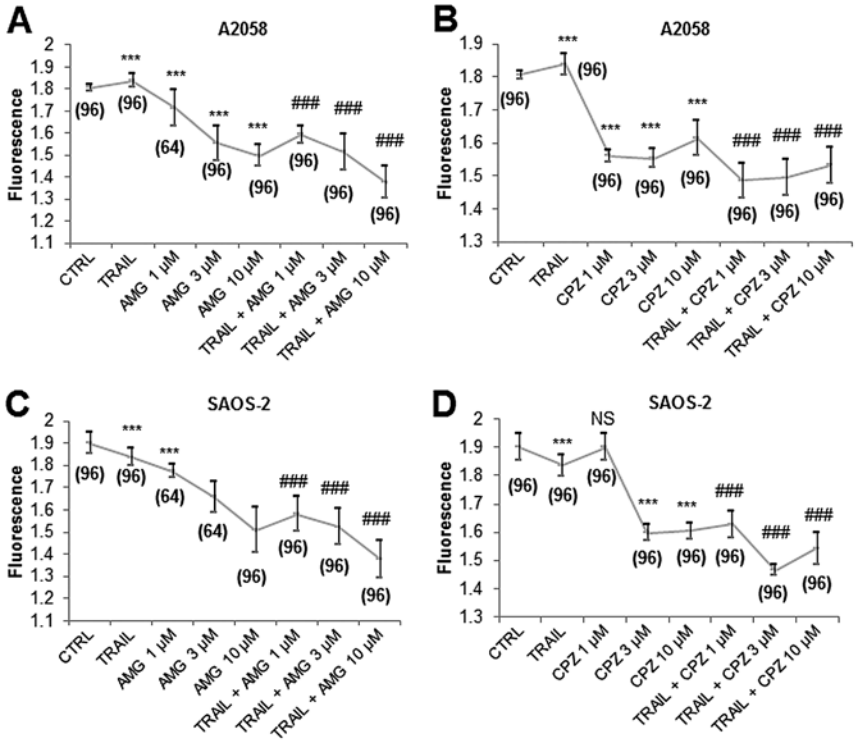


Figure 3. AMG9810 and capsazepine reduce $[Ca^{2+}]_{mit}$ cooperatively with TRAIL. Dihydrorhod 2-AM-loaded A2058 (A and B) and SAOS-2 cells (C and D) were suspended in the $Ca^{2+}$-containing medium in 96-well plates. The cells were added with 100 ng/ml TRAIL and AMG9810 or capsazepine at the indicated concentrations alone or in combination and measured for fluorescence at 5 sec intervals up to 3 min. The data show means ± SD in a representative experiment (N=3). Data were analyzed by ANOVA followed by the Tukey's post-hoc test. $^{***}$P<0.001; NS, not significant vs. control (CTRL). $^{###}$P<0.001 vs. TRAIL, AMG9810 or capsazepine alone. The number of parentheses represents the data analyzed.

a maximal effect at 1-3 $\mu$M (Fig. 3B). Essentially similar results were obtained for SAOS-2 cells (Fig. 3C and D). These results show that capsazepine and AMG9810 reduce $[Ca^{2+}]_{mit}$ cooperatively with TRAIL in MM and OS cells.

*$Ca^{2+}$ removal decreases MM and OS cell viability and potentiates TRAIL cytotoxicity*. To determine the role of $Ca^{2+}$ remodeling in TRAIL cytotoxicity toward MM and OS cells, we examined the effect of $Ca^{2+}$ removal on the cytotoxicity.

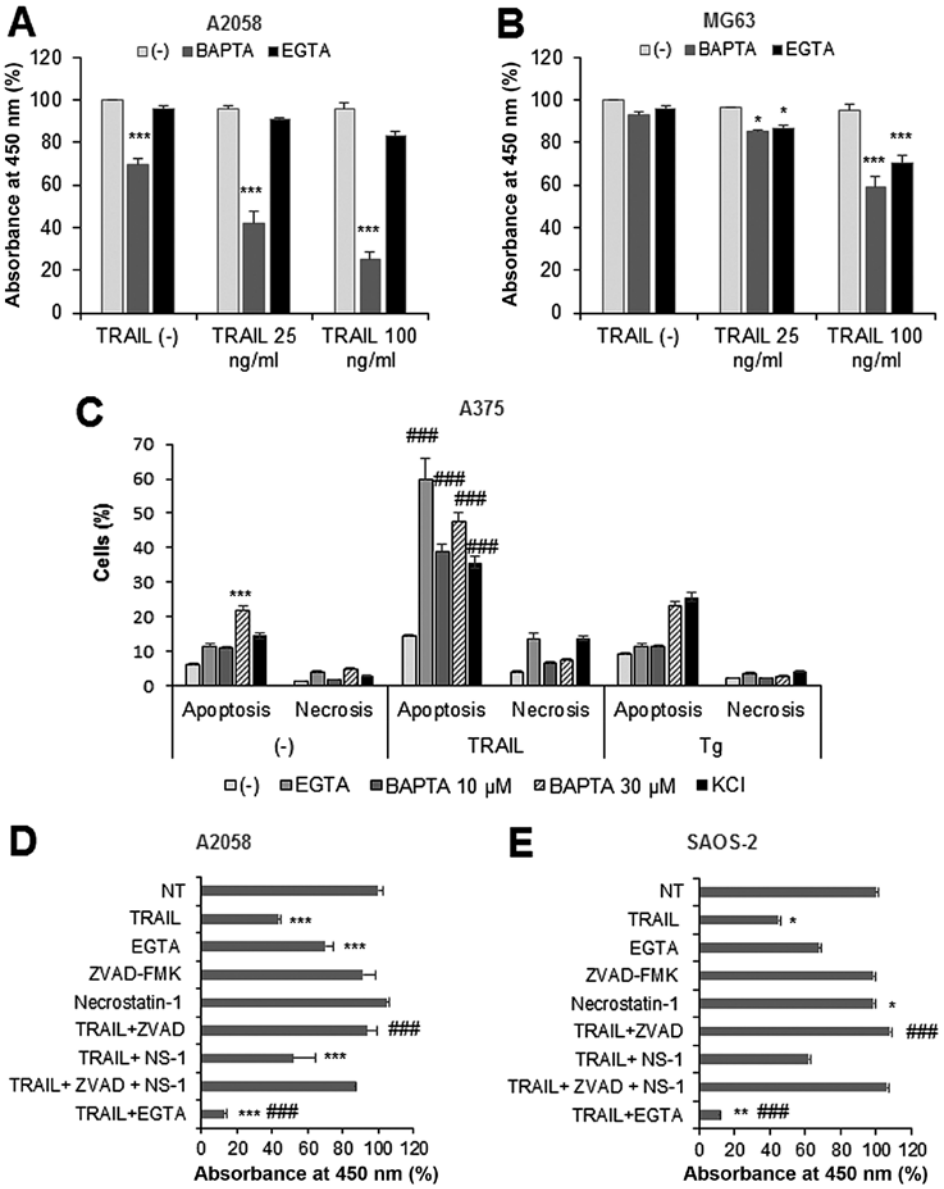


Figure 4. $Ca^{2+}$ removal decreases MM and OS cell viability and potentiates TRAIL cytotoxicity. A2058 (A) and MG63 (B) cells ($8x10^4$/well) were plated in 96-well plates and treated with 25 or 100 ng/ml TRAIL in the absence or presence of 30 $\mu$M BAPTA-AM (BAPTA) or 0.2 mM EGTA for 24 h and analyzed for viability using WST-8 assay in triplicates. The data show means ± SD for a representative experiment (N=3-5). (C) A375 cells were treated with 100 ng/ml TRAIL in the absence or presence of 0.2 mM EGTA, 10, 30 $\mu$M BAPTA, or 50 mM KCl for 24 h, and then analyzed for Annexin V/propidium iodide (PI) staining by flow cytometry. Annexin $V^+$ cells were considered to be apoptotic cells while Annexin $V^-/PI^+$ cells were regarded as necrotic cells. The data represent means ± SD from 3 independent experiments. A2058 (D) and SAOS-2 cells (E) were treated with 100 ng/ml TRAIL in the absence or presence of 30 $\mu$M BAPTA, 0.5 mM EGTA, 10 $\mu$M z-VAD-FMK (ZVAD), or 30 $\mu$M necrostatin-1 (NS-1) for 72 h and analyzed for viability using WST-8 assay in triplicates. The data show means ± SD for a representative experiment (N=3-5). Data were analyzed by ANOVA followed by the Tukey's post-hoc test. $^*P<0.05$; $^{**}P<0.01$; $^{***}P<0.001$; vs. control. $^{\#\#\#}P<0.001$ vs. TRAIL.

Treatment with TRAIL up to 100 ng/ml for 24 h minimally decreased (4-6% decrease) the viability of A2058 and MG63 cells. Treatment with the intracellular $Ca^{2+}$-chelator BAPTA (30 $\mu$M) moderately decreased the viability of A2058 cells (maximum of 30% reduction), while the extracellular $Ca^{2+}$-chelator EGTA (0.2-0.5 mM) had minimal effect (Fig. 4A), and both $Ca^{2+}$-chelators decreased the viability of MG63 cells only modestly (<10%) (Fig. 4B). BAPTA and EGTA sensitized both cells to TRAIL, and this effect became pronounced as the concentration was increased, although their effects varied depending on the cell lines tested (Fig. 4A and B).

To determine the cell death modality, we performed flow cytometric analyses using Annexin V/PI double staining. Likewise, KCl, a potent TRAIL-sensitizer (21), BAPTA or EGTA remarkably increased apoptotic (Annexin $V^+$) cells compared with TRAIL or either agent alone at 24 h (Fig. 4C). Small but significantly higher levels of necrotic (Annexin $V^-/PI^+$) cells were observed in TRAIL + EGTA-treated cells compared with TRAIL or EGTA alone (Fig. 4C). BAPTA and EGTA enhanced Tg-induced apoptosis, while had no significant effect on Tg-induced necrotic cell death. TRAIL toxicity, as well as TRAIL sensitization by the $Ca^{2+}$-chelators, became pronounced as the incubation period was prolonged. As a

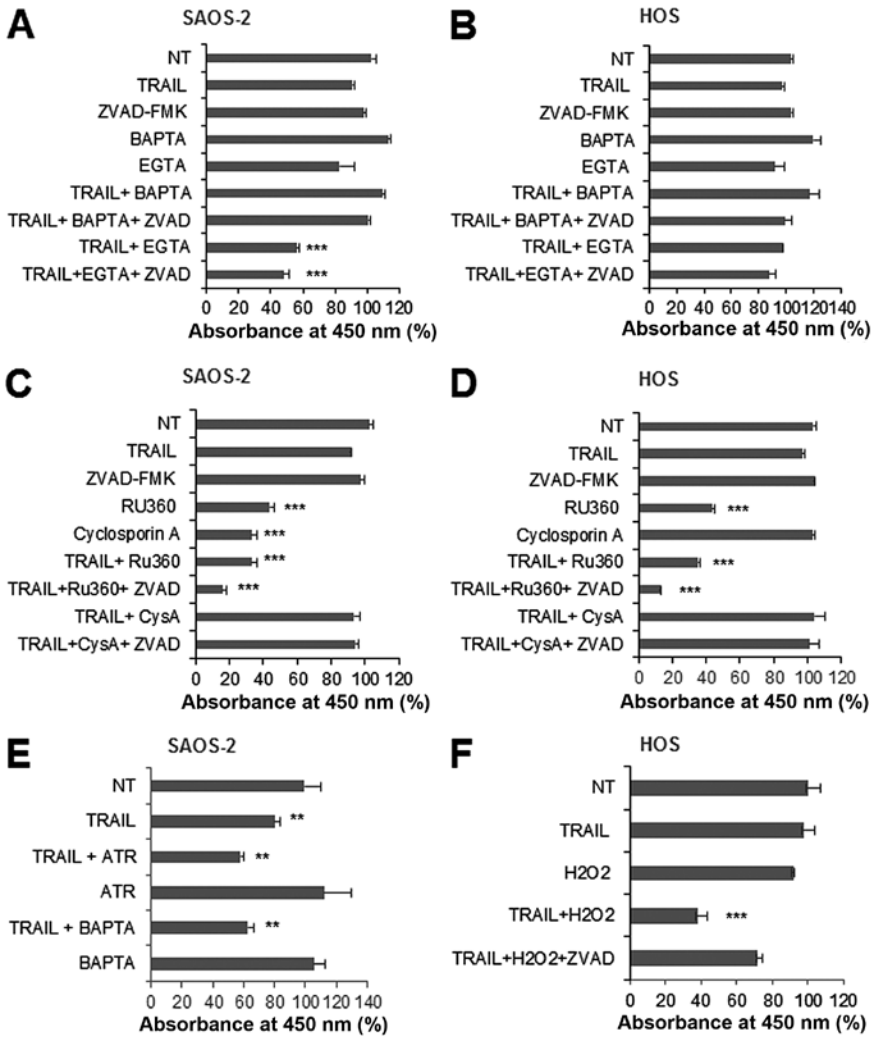


Figure 5. The potentiation of TRAIL cytotoxicity by $Ca^{2+}$ removal is caspase-independent. SAOS-2 (A, C and E) and HOS cells (B, D and F) were treated with 100 ng/ml TRAIL and 30 $\mu$M BAPTA, and 0.5 mM EGTA (A and B), 30 $\mu$M ruthenium 360 (Ru360) and 1 $\mu$M cyclosporin A (CysA) (C and D), 30 $\mu$M BAPTA and 5 $\mu$M atractyloside (ATR) (E), or 100 $\mu$M $H_2O_2$ (F) alone or in combination in the presence or absence of 10 $\mu$M z-VAD-FMK (ZVAD) for 72 h, and analyzed for viability using WST-8 assay in triplicates. The data show means ± SD in a representative experiment (N=3). Data were analyzed by ANOVA followed by the Tukey's post-hoc test. $^{**}P<0.01$; $^{***}P<0.001$ vs. non-treated control (NT).

result, TRAIL treatment for 72 h substantially decreased the viability of A2058 and SAOS-2 cells (56.4 and 54.8% reduction, respectively), while EGTA treatment alone reduced them moderately (30 and 32.2% reduction). When used together, TRAIL and EGTA considerably decreased cell viability (maximum of 90%) (Fig. 4D and E). The TRAIL cytotoxicity was entirely blocked by the pan-caspase-inhibitor z-VAD-FMK, while necrostatin-1, a specific inhibitor of necroptosis, had only a modest inhibitory effect, indicating that the TRAIL primarily induces apoptosis in these cells. Collectively, these results show that $Ca^{2+}$ removal sensitizes MM and OS cells to TRAIL-induced apoptosis, although the effect varied considerably depending on the cell line tested.

*$Ca^{2+}$ removal sensitizes MM and OS cells to TRAIL-induced non-apoptotic cell death*. The ability of TRAIL to kill MM and OS cells varied considerably in different experiments. Under certain conditions, TRAIL had the minimal cytotoxic effect toward SAOS-2 and HOS cells (Fig. 5A and B). These cells were resistant to the cytotoxic and TRAIL-sensitizing effects of the $Ca^{2+}$ chelators. As a result, TRAIL and chelator alone or in combination had the minimal cytotoxic effect except for that TRAIL + EGTA significantly reduced the viability of SAOS-2 cells (43.6% reduction). Also, z-VAD-FMK did not inhibit the effect of TRAIL + EGTA. Treatment with Ru360 (5-30 $\mu$M) for 24 h had the minimal cytotoxic and TRAIL-sensitizing effect (not shown). However, during another 48 h, Ru360 alone significantly decreased the viability of SAOS-2 and HOS cells (Fig. 5C and D). When Ru360 and TRAIL applied together, only a small increase of cell killing was observed compared with that induced by Ru360 alone. The cell death induced by Ru360 (not shown) or TRAIL + Ru360 was enhanced rather than inhibited by z-VAD-FMK (Fig. 5C and D). Although 5 $\mu$M CysA substantially decreased the viability of SAOS-2 cells, but not HOS cells, this cytotoxic effect was entirely counteracted by TRAIL. Moreover, atractyloside also enhanced TRAIL cytotoxicity in these apoptosis-resistant cells (Fig. 5E). On the other hand, consistent with our previous study with A375 cells (26), $H_2O_2$ markedly sensitized the cells to TRAIL cytotoxicity, and this

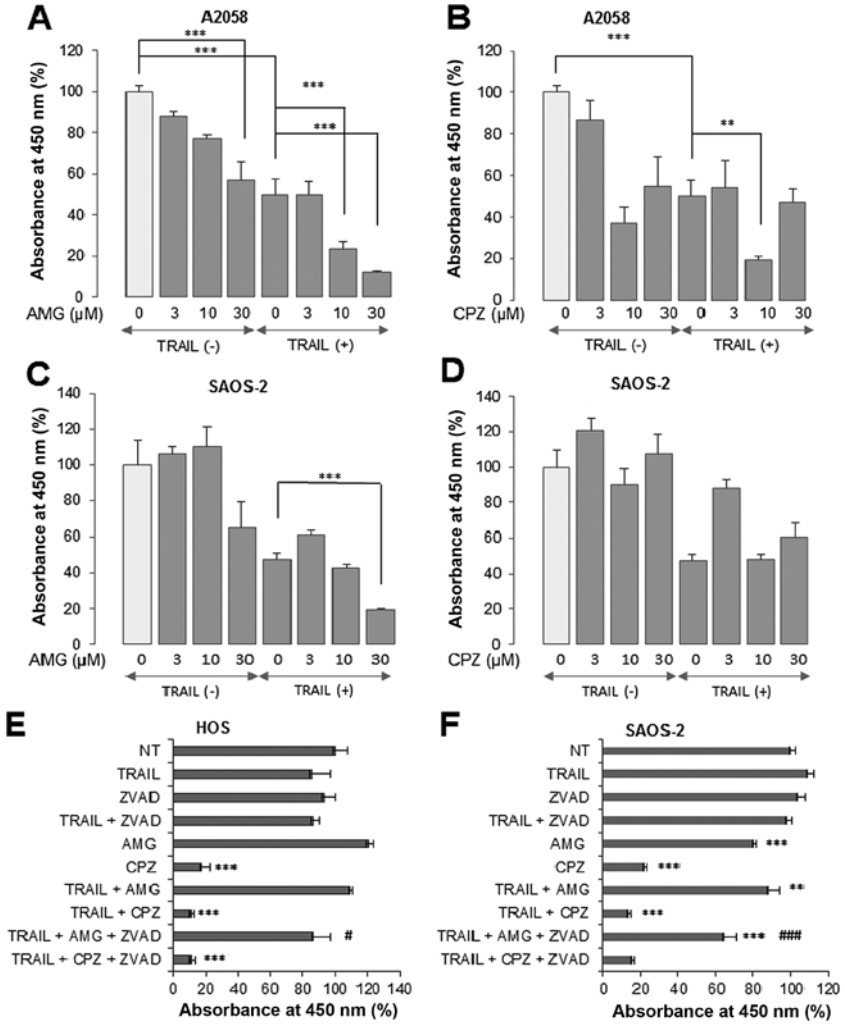


Figure 6. AMG9810 and capsazepine kill and sensitize MM and OS cells to a caspase-independent cell death. A2058 (A and B) and SAOS-2 cells (C and D) were treated with 100 ng/ml TRAIL and AMG9810 (A and C) or capsazepine (B and D) at the indicated concentrations alone or in combination for 72 h. HOS (E) and SAOS-2 cells (F) were treated with 100 ng/ml TRAIL and 10 $\mu$M each of AMG9810 or capsazepine alone or in combination in the presence or absence of 10 $\mu$M z-VAD-FMK (ZVAD) for 72 h. Then, the cells were analyzed for viability using WST-8 assay in triplicates. The data show means ± SD for a representative experiment (N=3). Data were analyzed by ANOVA followed by the Tukey's post-hoc test. $^{**}$P<0.01; $^{***}$P<0.001.

effect was completely blocked by z-VAD-FMK, indicating that $H_2O_2$ amplifies TRAIL-induced apoptosis. These results show that agents that reduce $[Ca^{2+}]_{mit}$ with different mechanisms of action sensitize these cells to TRAIL-induced non-apoptotic cell death.

*Capsazepine and AMG9810 kill or sensitize MM and OS cells in a caspase-independent manner.* To further explore the possible relationship between mitochondrial $Ca^{2+}$ removal and TRAIL sensitization, we assessed the impact of capsazepine and AMG9810 (3-30 $\mu$M) alone or in combination with TRAIL on tumor cell survival. Both AMG9810 and capsazepine had a minimal cytotoxic effect for 24 h (not shown). Treatment with AMG9810 at concentrations of ≥3 $\mu$M for 72 h reduced the viability of A2058 cells and at concentrations of ≥10 $\mu$M potentiated TRAIL cytotoxicity toward them in a dose-dependent manner (Fig. 6A). SAOS-2 cells were more resistant to AMG9810 treatment so that only the highest concentration of the agent exhibited substantial cytotoxic effect and enhanced TRAIL cytotoxicity (Fig. 6C). The effect of capsazepine seemed to be complicated and dependent on the cell lines tested. Capsazepine (10 $\mu$M) was more cytotoxic and more efficient in potentiating TRAIL cytotoxicity than 30 $\mu$M capsazepine in A2058 cells (Fig. 6B) while exhibiting no significant cytotoxicity nor TRAIL-sensitizing effect in SAOS-2 cells (Fig. 6D). Usually, HOS cells were highly resistant to TRAIL and AMG9810 alone or in combination, and the cytotoxic effect of TRAIL + AMG9810 was significantly augmented by z-VAD-FMK (Fig. 6E). On the other hand, capsazepine alone decreased their viability remarkably (82.9% reduction), and the effect was comparable to that of TRAIL + capsazepine. z-VAD-FMK also enhanced the cytotoxic effect of TRAIL + AMG9810 in SAOS-2 cells (Fig. 6F).

*Capsazepine and AMG9810 initially amplify TRAIL-induced caspase-3/7 activation and cell membrane damage in MM and OS cells.* The results presented so far suggested that capsazepine and AMG9810 potentiate TRAIL cytotoxicity in a caspase-independent manner. To determine whether these two agents indeed modulate cell death independently of apoptosis, we examined their effect on caspase-3/7 activation. We simultaneously assessed caspase-3/7 activation and cell membrane

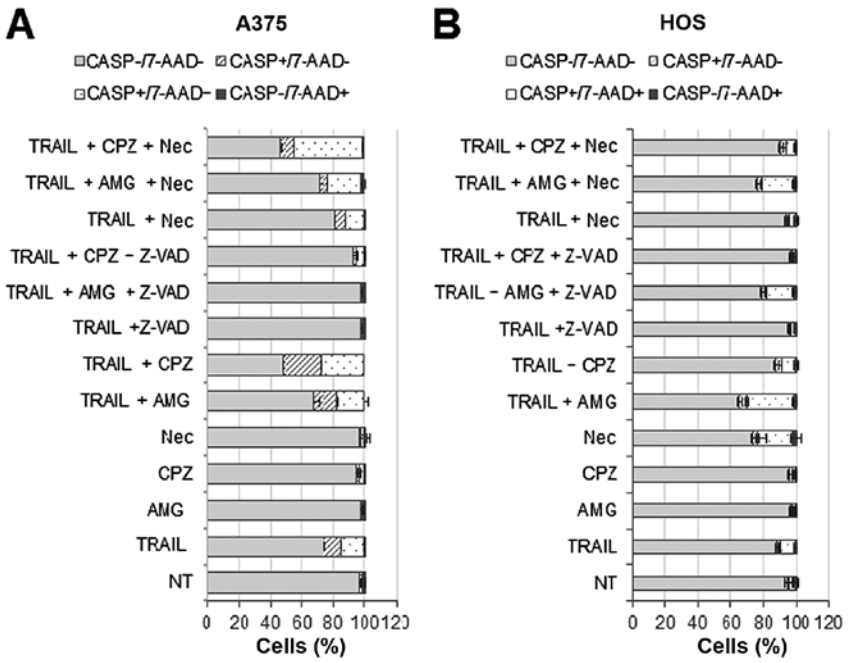


Figure 7. AMG9810 and capsazepine potentiate TRAIL-induced caspase-3/7 activation and cell membrane damage in the early stage. A375 (A) and HOS cells (B) ($1x10^5$/ml) in 24-well plates were treated with 100 ng/ml TRAIL, 30 $\mu$M each of AMG9810 and capsazepine alone or in combination the absence or presence of 10 $\mu$M z-VAD-FMK (ZVAD) or 30 $\mu$M necrostatin-1 (Nec) for 24 h. Then, the cells were stained with a caspase-3/7 reagent NucView™ and 7-amino-actinomycin D (7-AAD) and analyzed for caspase-3/7 activation, membrane integrity, and cell death using Muse™ Cell Analyzer. Four populations of cells can be distinguished by this method; Live cells: caspase-3/7 $(CASP)^-$7-$AAD^-$; early apoptotic cells: $CASP^+$/7-$AAD^-$; late apoptotic/dead cells: $CASP^+$/7-$AAD^+$; necrotic cells: $CASP^-$/7-$AAD^+$. The data show means ± SD for a representative experiment (N=3).

damage/death by using a caspase-3/7-specific substrate and 7-AAD, respectively. The latter is a nucleus-staining dye, which is excluded by healthy cells, while it can penetrate cell membranes of dying or dead cells. Results showed that in A375 cells, capsazepine and AMG9810 alone minimally increased caspase-3/7 activated (caspase$^+$) cells and damaged (7-$AAD^+$) cells at 24 h (Fig. 7A). TRAIL treatment modestly increased both caspase$^+$/7-$AAD^-$ and caspase$^+$/7-$AAD^+$ cells in A375 cells, and z-VAD-FMK blocked this effect. Capsazepine, and to a lesser extent, AMG9810 potentiated the effect of TRAIL, and z-VAD-FMK also abrogated the amplification (Fig. 7A). Necrostatin-1 inhibited the effect of TRAIL only modestly, while reducing the increase in caspase$^+$/7-$AAD^-$ cells, but not caspase$^+$/7-$AAD^+$ cells by TRAIL + AMG9810. Strikingly, necrostain-1 enhanced the increase in caspase$^+$/7-$AAD^+$ cells by TRAIL + capsazepine (Fig. 7A). On the other hand, in HOS cells, AMG9810 was more potent than capsazepine in potentiating the effect of TRAIL, and z-VAD-FMK blocked the effect of capsazepine and AMG9810 (Fig. 7B). Unlike A375 cells, necrostatin-1 alone moderately increased caspase$^+$/7-$AAD^+$ cells while blunting the rise in such cell population by TRAIL, TRAIL + AMG9810, or TRAIL + capsazepine (Fig. 7B). These results indicate that capsazepine and AMG9810 initially amplify TRAIL-induced caspase-3/7 activation, cell membrane damage, and caspase-dependent cell death depending on the cell types.

## Discussion

In the present study, we analyzed the effect of TRAIL on $Ca^{2+}$ dynamics in MM and OS cells and the possible role of $Ca^{2+}$ in the control of their survival and TRAIL sensitivity. Our results revealed that acute TRAIL treatment modulates $Ca^{2+}$ remodeling in an array of MM and OS cell lines, as indicated by a rapid and persistent increase in $[Ca^{2+}]_{cyt}$ and $[Ca^{2+}]_{mit}$ (Fig. 1A-D). In parallel with its cytotoxicity, TRAIL increased $Ca^{2+}$ levels at the two intracellular sites in a dose-dependent manner. The mitochondria take up or release $Ca^{2+}$ depending on $[Ca^{2+}]_{cyt}$, thereby serving as a critical intracellular $Ca^{2+}$ reservoir that maintains $[Ca^{2+}]_{cyt}$. According to this paradigm, the increases in $[Ca^{2+}]_{cyt}$ and $[Ca^{2+}]_{mit}$ may occur in parallel. Strikingly, however, the rise in $[Ca^{2+}]_{cyt}$ was usually dose-dependent while depending on the cellular conditions, the elevation in $[Ca^{2+}]_{mit}$ was maximum at 50 ng/ml, and higher concentrations of TRAIL had a smaller effect. These findings indicate that the mitochondrial $Ca^{2+}$ responses involve both $[Ca^{2+}]_{cyt}$-dependent and $[Ca^{2+}]_{cyt}$-independent processes. Mitochondrial $Ca^{2+}$ homeostasis is maintained by a well-balanced mitochondrial $Ca^{2+}$ uptake and efflux. The MCU complex consists of the channel-forming subunit of the uniporter MCU and multiple components such as MICU1/2, MCUb, MCUR1, and EMRE. These complex molecules are proven to be an essential mitochondrial $Ca^{2+}$ uptake machinery in different cell types including cancer cells (26-28).

The mitochondrion releases $Ca^{2+}$ through several different pathways including NCLX, $Ca^{2+}/H^+$ antiporter (29) and MPTP (30-33). However, the role of MPTP is still a matter of debate, because other observations suggest its minimal contribution to mitochondrial $Ca^{2+}$ extrusion (34). In this study, we showed that the MCU inhibitor Ru360 decreased $[Ca^{2+}]_{mit}$, while the NCLX antagonist CGP-37157 increased it in MM

and OS cells (Fig. 2A and B). The results indicate that $Ca^{2+}$ uptake through MCU and $Ca^{2+}$ extrusion through NCLX are key regulators of $[Ca^{2+}]_{mit}$ in our cell systems. Cyclosporine A, which targets cyclophilin D, a critical component of the MPTP opening (32,33), affected $[Ca^{2+}]_{mit}$ in some but not all cell types. Whereas, atractyloside, which opens MPTP by modulating adenine nucleotide translocator (34), reduced $[Ca^{2+}]_{mit}$ in different cell types (Fig. 2C and D). These findings suggest that $Ca^{2+}$ extrusion through MPTP is also necessary for the control of $[Ca^{2+}]_{mit}$, yet cyclophilin D plays a dispensable role in the MPTP opening in our cell systems as previously reported by other groups (35,36).

It is noteworthy that capsazepine and AMG9810 markedly reduce $[Ca^{2+}]_{mit}$ and potentiate TRAIL-induced drop in $[Ca^{2+}]_{mit}$ in MM and OS cells (Fig. 3A-D). These findings indicate that a $Ca^{2+}$ transport pathway sensitive to these agents plays a pivotal role in regulating $[Ca^{2+}]_{mit}$ in them. The two agents are known to act as potent antagonists of TRPV1 (37,38), a molecule which localizes to the plasma membrane and serves as a non-selective cation channel. Recently, TRPV1 was shown to also exist in the ER and mitochondria in non-transformed cells and cancer cells. The intracellular TRPV1 contributes to $Ca^{2+}$ release and ER stress (39-41). These facts suggest a close functional relationship among this channel, ER, and mitochondria in the regulation of $Ca^{2+}$ signaling and survival of cancer cells. It is now widely accepted that ROS and $Ca^{2+}$ mutually regulate one another and cooperatively control cell survival and death (13). Several groups, including us, have previously demonstrated that ROS plays a critical role in TRAIL cytotoxicity toward different malignant cell types (42-44).

Moreover, TRPV1 is one of TRP channels that are activated by ROS (45). Collectively, TRPV1 might play a role in the regulation of $Ca^{2+}$ dynamics, survival, and death of MM and OS cells. However, to date, the role of TRPV1 in the control of $Ca^{2+}$ in MM and OS is poorly documented. Mergler *et al* (46) reported the expression of TRPV1 in human uveal melanoma cells and $Ca^{2+}$ regulation by it. The TRPV1 agonist capsaicin is shown to induce an increase in $[Ca^{2+}]_{mit}$ in G292 human OS cells independently of the extracellular $Ca^{2+}$ and depletion of intracellular $Ca^{2+}$ (47). Since the extracellular $Ca^{2+}$ entry appears to be dispensable for increasing $[Ca^{2+}]_{mit}$ (Fig. 2A and B), an intracellular TRPV1 might play a role in the regulation of $[Ca^{2+}]_{mit}$ homeostasis. However, at present, we failed to detect any TRPV1 in the intracellular sites in these cells (data not shown). Thus, the occurrence and the role of TRPV1 remain to be studied.

Another significant finding in this study was that depletion of $Ca^{2+}$ potentiated TRAIL cytotoxicity toward MM and OS cells (Figs. 4 and 5). The finding strongly suggests that $Ca^{2+}$ protects them from cell death. Both intracellular and extracellular $Ca^{2+}$ seemed to play a role in this pro-survival function while the position of the two $Ca^{2+}$ varied depending on cell lines. Depletion of $Ca^{2+}$ enhanced apoptotic, but not necrotic cell death induced by TRAIL and Tg (Fig. 4C), indicating that $Ca^{2+}$ primarily prevents apoptosis. It is noteworthy that the effect of $Ca^{2+}$ removal was more pronounced in TRAIL-sensitive cells than in TRAIL-resistant cells (compare Fig. 4 with Fig. 5), and that z-VAD-FMK blocked the effect in the TRAIL-sensitive cells, but not in TRAIL-resistant cells. Collectively, MM and OS cells may each have distinct cellular statuse with different TRAIL sensitivity. One is relatively TRAIL-sensitive status, where they readily undergo apoptosis in response to TRAIL. The other is TRAIL-resistant status where another non-apoptotic cell death is necessary for efficient cell killing because only a small cell population undergo apoptosis. $Ca^{2+}$ removal also potentiated TRAIL-induced non-apoptotic cell death (Fig. 5), indicating that $Ca^{2+}$ also prevents this cell death modality.

The data presented in this study revealed the critical role of mitochondrial $Ca^{2+}$ in the prevention of cell death. We found that the reduction in $[Ca^{2+}]_{mit}$ by inhibiting $Ca^{2+}$ uptake through MCU sensitized MM and OS cells to TRAIL-induced non-apoptotic cell death (Fig. 5). The finding is consistent with several recent studies in other cancer cell types. Curry and colleagues (27) reported that MCU silencing potentiates caspase-independent cell death in MDA-MB-231 breast cancer cells. The authors demonstrated that caspase-independent cell death induced by the $Ca^{2+}$-ionophore ionomycin is potentiated by MCU silencing whereas caspase-dependent cell death caused by Bcl-2 inhibition is unaffected. Moreover, the potentiation of caspase-independent cell death occurs independently of overall $[Ca^{2+}]_{cyt}$ changes.

Marchi *et al* (48) reported that the *in silico* microRNA miR-25 downregulates MCU expression and reduces mitochondrial $Ca^{2+}$ uptake in HeLa cells and colon cancer cells and that this downregulation correlates with resistance to apoptotic stimuli. In this case, this MCU manipulation does not affect $[Ca^{2+}]_{cyt}$. Moreover, we found that the inhibition of a $Ca^{2+}$ transport pathway by capsazepine and AMG9810 led to the decrease in $[Ca^{2+}]_{mit}$ (Fig. 3) and sensitized MM and OS cells to TRAIL-induced non-apoptotic cell death. Strikingly, capsazepine and AMG9810 eventually amplified cell killing in a caspase-independent manner (Fig. 6) while initially (within 24 h) potentiated TRAIL-induced caspase-3/7 activation and apoptosis (Fig. 8). The reduction in $[Ca^{2+}]_{mit}$ by promoting $Ca^{2+}$ extrusion through MPTP also amplified TRAIL cytotoxicity (Fig. 5), providing further support for the pro-survival role of mitochondrial $Ca^{2+}$. TRAIL was recently shown to induce necroptosis, the programmed necrotic cell death (10,11). However, the $Ca^{2+}$ modulation had the minimal effect on necrosis (Fig. 4) and necrostatin-1, a specific inhibitor of necroptosis, had no or only a modest inhibitory effect on the cell death induced by TRAIL (Fig. 4), TRAIL + capsazepine, and TRAIL + AMG9810 (Fig. 7). These findings suggest that necroptosis plays a minor role in the cell killing yet the silencing of an essential molecular component in this cell death modality such as receptor-interacting protein 1/3 may be necessary to verify this view.

In conclusion, we demonstrate in this study that mitochondrial $Ca^{2+}$ acts as a pro-survival factor in MM and OS cells by preventing apoptosis and non-apoptotic cell death. The findings suggest that mitochondrial $Ca^{2+}$ may serve as a promising target for overcoming the resistance of these cancers to TRAIL.

## Acknowledgements

The authors thank Drs T. Ito, T. Tokunaga, and A. Onoe for their technical assistance. This work was supported in part by JSPS KAKENHI grant no. 15K09750 to Y.S-K.).

## References


1. Ivanov VN, Bhoumik A and Ronai Z: Death receptors and melanoma resistance to apoptosis. Oncogene 22: 3152-3161, 2003.
2. Guiho R, Biteau K, Heymann D and Redini F: TRAIL-based therapy in pediatric bone tumors: How to overcome resistance. Future Oncol 11: 535-542, 2015.
3. Ashkenazi A: Targeting the extrinsic apoptosis pathway in cancer. Cytokine Growth Factor Rev 19: 325-331, 2008.
4. Amarante-Mendes GP and Griffith TS: Therapeutic applications of TRAIL receptor agonists in cancer and beyond. Pharmacol Ther 155: 117-131, 2015.
5. de Miguel D, Lemke J, Anel A, Walczak H and Martinez-Lostao L: Onto better TRAILs for cancer treatment. Cell Death Differ 23: 733-747, 2016.
6. Wang S: The promise of cancer therapeutics targeting the TNF-related apoptosis-inducing ligand and TRAIL receptor pathway. Oncogene 27: 6207-6215, 2008.
7. Sayers TJ: Targeting the extrinsic apoptosis signaling pathway for cancer therapy. Cancer Immunol Immunother 60: 1173-1180, 2011.
8. Herrero-Martín G, Høyer-Hansen M, García-García C, Fumarola C, Farkas T, López-Rivas A and Jäättelä M: TAK1 activates AMPK-dependent cytoprotective autophagy in TRAIL-treated epithelial cells. EMBO J 28: 677-685, 2009.
9. He W, Wang Q, Xu J, Xu X, Padilla MT, Ren G, Gou X and Lin Y: Attenuation of TNFSF10/TRAIL-induced apoptosis by an autophagic survival pathway involving TRAF2- and RIPK1/RIP1-mediated MAPK8/JNK activation. Autophagy 8: 1811-1821, 2012.
10. Jouan-Lanhouet S, Arshad MI, Piquet-Pellorce C, Martin-Chouly C, Le Moigne-Muller G, Van Herreweghe F, Takahashi N, Sergent O, Lagadic-Gossmann D, Vandenabeele P, *et al*: TRAIL induces necroptosis involving RIPK1/RIPK3-dependent PARP-1 activation. Cell Death Differ 19: 2003-2014, 2012.
11. Sosna J, Philipp S, Fuchslocher Chico J, Saggau C, Fritsch J, Föll A, Plenge J, Arenz C, Pinkert T, Kalthoff H, *et al*: Differences and similarities in TRAIL- and tumor necrosis factor-mediated necroptotic signaling in cancer cells. Mol Cell Biol 36: 2626-2644, 2016.
12. Dimberg LY, Anderson CK, Camidge R, Behbakht K, Thorburn A and Ford HL: On the TRAIL to successful cancer therapy? Predicting and counteracting resistance against TRAIL-based therapeutics. Oncogene 32: 1341-1350, 2013.
13. Hempel N and Trebak M: Crosstalk between calcium and reactive oxygen species signaling in cancer. Cell Calcium: Jan 18, 2017 (Epub ahead of print).
14. Villalobos C, Sobradillo D, Hernández-Morales M and Núñez L: Calcium remodeling in colorectal cancer. Biochim Biophys Acta 1864: 843-849, 2017.
15. Danese A, Patergnani S, Bonora M, Wieckowski MR, Previati M, Giorgi C and Pinton P: Calcium regulates cell death in cancer: Roles of the mitochondria and mitochondria-associated membranes (MAMs). Biochim Biophys Acta: Jan 10, 2017 (Epub ahead of print).
16. Nilius B and Szallasi A: Transient receptor potential channels as drug targets: From the science of basic research to the art of medicine. Pharmacol Rev 66: 676-814, 2014.
17. Orrenius S, Gogvadze V and Zhivotovsky B: Calcium and mitochondria in the regulation of cell death. Biochem Biophys Res Commun 460: 72-81, 2015.
18. Storr SJ, Carragher NO, Frame MC, Parr T and Martin SG: The calpain system and cancer. Nat Rev Cancer 11: 364-374, 2011.
19. Moretti D, Del Bello B, Allavena G and Maellaro E: Calpains and cancer: Friends or enemies? Arch Biochem Biophys 564: 26-36, 2014.
20. Akita M, Suzuki-Karasaki M, Fujiwara K, Nakagawa C, Soma M, Yoshida Y, Ochiai T, Tokuhashi Y and Suzuki-Karasaki Y: Mitochondrial division inhibitor-1 induces mitochondrial hyperfusion and sensitizes human cancer cells to TRAIL-induced apoptosis. Int J Oncol 45: 1901-1912, 2014.
21. Suzuki Y, Inoue T, Murai M, Suzuki-Karasaki M, Ochiai T and Ra C: Depolarization potentiates TRAIL-induced apoptosis in human melanoma cells: Role for ATP-sensitive $K^+$ channels and endoplasmic reticulum stress. Int J Oncol 41: 465-475, 2012.
22. Suzuki Y, Yoshimaru T, Inoue T and Ra C: Mitochondrial $Ca^{2+}$ flux is a critical determinant of the $Ca^{2+}$ dependence of mast cell degranulation. J Leukoc Biol 79: 508-518, 2006.
23. Marchi S and Pinton P: The mitochondrial calcium uniporter complex: Molecular components, structure and physiopathological implications. J Physiol 592: 829-839, 2014.
24. Tosatto A, Sommaggio R, Kummerow C, Bentham RB, Blacker TS, Berecz T, Duchen MR, Rosato A, Bogeski I, Szabadkai G, *et al*: The mitochondrial calcium uniporter regulates breast cancer progression via HIF-1α. EMBO Mol Med 8: 569-585, 2016.
25. Yang X, Wang B, Zeng H, Cai C, Hu Q, Cai S, Xu L, Meng X and Zou F: Role of the mitochondrial $Ca^{2+}$ uniporter in $Pb^{2+}$-induced oxidative stress in human neuroblastoma cells. Brain Res 1575: 12-21, 2014.
26. Tochigi M, Inoue T, Suzuki-Karasaki M, Ochiai T, Ra C and Suzuki-Karasaki Y: Hydrogen peroxide induces cell death in human TRAIL-resistant melanoma through intracellular superoxide generation. Int J Oncol 42: 863-872, 2013.
27. Curry MC, Peters AA, Kenny PA, Roberts-Thomson SJ and Monteith GR: Mitochondrial calcium uniporter silencing potentiates caspase-independent cell death in MDA-MB-231 breast cancer cells. Biochem Biophys Res Commun 434: 695-700, 2013.
28. De Stefani D, Patron M and Rizzuto R: Structure and function of the mitochondrial calcium uniporter complex. Biochim Biophys Acta 1853: 2006-2011, 2015.
29. Brand MD: Electroneutral efflux of $Ca^{2+}$ from liver mitochondria. Biochem J 225: 413-419, 1985.
30. Altschuld RA, Hohl CM, Castillo LC, Garleb AA, Starling RC and Brierley GP: Cyclosporin inhibits mitochondrial calcium efflux in isolated adult rat ventricular cardiomyocytes. Am J Physiol 262: H1699-H1704, 1992.
31. Bernardi P and von Stockum S: The permeability transition pore as a $Ca^{2+}$ release channel: New answers to an old question. Cell Calcium 52: 22-27, 2012.
32. Di Lisa F, Carpi A, Giorgio V and Bernardi P: The mitochondrial permeability transition pore and cyclophilin D in cardioprotection. Biochim Biophys Acta 1813: 1316-1322, 2011.
33. Gutiérrez-Aguilar M and Baines CP: Structural mechanisms of cyclophilin D-dependent control of the mitochondrial permeability transition pore. Biochim Biophys Acta 1850: 2041-2047, 2015.
34. Klingenberg M: The ADP and ATP transport in mitochondria and its carrier. Biochim Biophys Acta 1778: 1978-2021, 2008.
35. Zamorano S, Rojas-Rivera D, Lisbona F, Parra V, Court FA, Villegas R, Cheng EH, Korsmeyer SJ, Lavandero S and Hetz C: A BAX/BAK and cyclophilin D-independent intrinsic apoptosis pathway. PLoS One 7: e37782, 2012.
36. Briston T, Lewis S, Koglin M, Mistry K, Shen Y, Hartopp N, Katsumata R, Fukumoto H, Duchen MR, Szabadkai G, *et al*: Identification of ER-000444793, a Cyclophilin D-independent inhibitor of mitochondrial permeability transition, using a high-throughput screen in cryopreserved mitochondria. Sci Rep 6: 37798, 2016.
37. Bevan S, Hothi S, Hughes G, James IF, Rang HP, Shah K, Walpole CS and Yeats JC: Capsazepine: A competitive antagonist of the sensory neurone excitant capsaicin. Br J Pharmacol 107: 544-552, 1992.
38. Gavva NR, Tamir R, Qu Y, Klionsky L, Zhang TJ, Immke D, Wang J, Zhu D, Vanderah TW, Porreca F, *et al*: AMG 9810 [(E)-3-(4-t-butylphenyl)-N-(2,3-dihydrobenzo[b][1,4] dioxin-6-yl)acrylamide], a novel vanilloid receptor 1 (TRPV1) antagonist with antihyperalgesic properties. J Pharmacol Exp Ther 313: 474-484, 2005.
39. Zhao R and Tsang SY: Versatile roles of intracellularly located TRPV1 channel. J Cell Physiol 232: 1957-1965, 2017.
40. Thomas KC, Roberts JK, Deering-Rice CE, Romero EG, Dull RO, Lee J, Yost GS and Reilly CA: Contributions of TRPV1, endovanilloids, and endoplasmic reticulum stress in lung cell death in vitro and lung injury. Am J Physiol Lung Cell Mol Physiol 302: L111-L119, 2012.
41. Stock K, Kumar J, Synowitz M, Petrosino S, Imperatore R, Smith ES, Wend P, Purfürst B, Nuber UA, Gurok U, *et al*: Neural precursor cells induce cell death of high-grade astrocytomas through stimulation of TRPV1. Nat Med 18: 1232-1238, 2012.
42. Mellier G and Pervaiz S: The three Rs along the TRAIL: Resistance, re-sensitization and reactive oxygen species (ROS). Free Radic Res 46: 996-1003, 2012.
43. Suzuki-Karasaki M, Ochiai T and Suzuki-Karasaki Y: Crosstalk between mitochondrial ROS and depolarization in the potentiation of TRAIL-induced apoptosis in human tumor cells. Int J Oncol 44: 616-628, 2014.

44. Voltan R, Secchiero P, Casciano F, Milani D, Zauli G and Tisato V: Redox signaling and oxidative stress: Cross talk with TNF-related apoptosis inducing ligand activity. Int J Biochem Cell Biol 81: 364-374, 2016.
45. Kozai D, Ogawa N and Mori Y: Redox regulation of transient receptor potential channels. Antioxid Redox Signal 21: 971-986, 2014.
46. Mergler S, Derckx R, Reinach PS, Garreis F, Böhm A, Schmelzer L, Skosyrski S, Ramesh N, Abdelmessih S, Polat OK, *et al*: Calcium regulation by temperature-sensitive transient receptor potential channels in human uveal melanoma cells. Cell Signal 26: 56-69, 2014.
47. Chien CS, Ma KH, Lee HS, Liu PS, Li YH, Huang YS and Chueh SH: Dual effect of capsaicin on cell death in human osteosarcoma G292 cells. Eur J Pharmacol 718: 350-360, 2013.
48. Marchi S, Lupini L, Patergnani S, Rimessi A, Missiroli S, Bonora M, Bononi A, Corrà F, Giorgi C, De Marchi E, *et al*: Downregulation of the mitochondrial calcium uniporter by cancer-related miR-25. Curr Biol 23: 58-63, 2013.